

Attribution of satellite observed vegetation trends in a hyper-arid region of the Heihe River Basin, Central Asia

Y. Wang^{1,2,3,4}, M. L. Roderick^{4,5,6}, Y. Shen¹, F. Sun^{4,6}

¹ Key Laboratory of Agricultural Water Resources, Hebei Key Laboratory of Agricultural Water-Saving, Center for Agricultural Resources Research, Institute of Genetics and Developmental Biology, Chinese Academy of Sciences, Shijiazhuang 050021, China

² University of Chinese Academy of Sciences, Beijing 10049, China

³ Research center for Hebei Ecological Environmental Construction, Hebei Academy of Social Sciences, Shijiazhuang 050051, China

⁴ Research School of Biology, The Australian National University, Canberra 0200, Australia

⁵ Research School of Earth Science, The Australian National University, Canberra 0200, Australia

⁶ Australian Research Council Centre of Excellence for Climate System Science

Correspondence to: Y. J. Shen (yjshen@sjziam.ac.cn)

Abstract

Terrestrial vegetation dynamics are closely influenced by both climate and by direct human activities that modify land use and/or land cover (LULCC). Both can change over time in a monotonic way and it can be difficult to separate the effects of climate change from LULCC on vegetation. Here we attempt to attribute trends in the fractional green vegetation cover to climate variability and to human activity in Ejina region, a hyper-arid landlocked region in northwest China. This region is dominated by extensive deserts with relatively small areas of irrigation located along the major water courses as is typical throughout much of Central Asia. Variations of fractional vegetation cover from 2000 to 2012 were determined using Moderate Resolution Imaging Spectroradiometer (MODIS) vegetation index data with 250m spatial resolution over 16-day intervals. We found that the fractional vegetation cover in this hyper-arid region is very low, but that the mean growing season vegetation cover has increased from 3.4% in 2000 to 4.5% in 2012. The largest contribution to the overall greening was due to changes in green vegetation cover of the extensive desert areas with a smaller

1 contribution due to changes in the area of irrigated land. Comprehensive analysis with
2 different precipitation data sources found that the greening of the desert was associated with
3 increases in regional precipitation. We further report that the area of land irrigated each year
4 could be predicted using the runoff gauged one year earlier. Taken together, water availability
5 both from precipitation in the desert and runoff inflow for the irrigation agricultural lands can
6 explain at least 52% of the total variance in regional vegetation cover from 2000 to 2010. The
7 results demonstrate that it is possible to separate the satellite-observed changes in green
8 vegetation cover into components due to climate and due to human modifications. Such
9 results inform management on the implications for water allocation between oases in middle
10 and lower reaches and for water management in the Ejina oasis.

11 **1 Introduction**

12 Terrestrial vegetation plays a key role in energy, water and biogeochemical cycles and
13 changes in vegetation can also significantly influence atmospheric processes (Pielke et al.,
14 1998; Gerten et al., 2004). Monitoring of terrestrial vegetation dynamics therefore underpins
15 efforts to better understand the feedbacks between vegetation and the atmosphere (Bonan et
16 al., 2003; Bounoua et al., 2010; Angelini et al., 2011). In particular, the Normalized
17 Difference Vegetation Index (NDVI) derived from satellite observations of red and
18 near-infrared reflectance has proven useful in assessing vegetation dynamics from regional to
19 global scales (Tucker, 1979; Box et al., 1989; Fensholt et al., 2013).

20 Greening trends have been detected on global (Myneni et al., 1997; Nemani et al., 2003;
21 Donohue et al., 2013; Fensholt et al., 2013) and regional (Fang et al., 2004; Herrmann et al.,
22 2005; Donohue et al., 2009) scales but attribution of those trends in terms of the underlying
23 biophysical and socio-economic causes remains a difficult task. The central challenge is that
24 vegetation can change for a myriad of reasons including changes in the local climate (e.g.,
25 rainfall, radiation, temperature, humidity, etc.) (Myneni et al., 1997; Goetz et al., 2005;
26 Donohue et al., 2009), biogeochemistry (e.g., atmospheric CO₂, nutrient deposition, etc.) (Lim
27 et al., 2004; Bond et al., 2003; Donohue et al., 2013; Dirnböck et al., 2014), ecological
28 processes (e.g. long term successional recovery from disturbance, fire dynamics, disease, etc.)
29 (Thonicke et al., 2001; Bond et al., 2003) and via direct anthropogenic activity (e.g., land use
30 change, irrigation, agriculture, etc.) (Hutchinson et al., 2000; Thonicke et al., 2001). One
31 approach to handle this complexity is to use regional knowledge to constrain the problem.

1 In terms of the attribution of regional vegetation trends, Central Asia presents a unique
2 challenge. The region is hyper-arid with annual precipitation in many areas often less than 50
3 mm with hot summers and cold winters. What is of particular interest throughout Central Asia
4 is the presence of many localised regions of irrigated agriculture that often support relatively
5 large local populations. Those irrigation communities are usually located at oases that receive
6 an annual input of water in the form of runoff from surrounding mountains. Much of the
7 outflow from the mountains is recent precipitation (snow-melt) but a further complication of
8 recent years is that glacier melt has augmented the snow melt and increased inflow of water to
9 many oases throughout Central Asia (Yao et al., 2004; Lioubimtseva and Henebry, 2009;
10 Rahimov, 2009; Unger-Shayesteh et al., 2013). Time series of NDVI satellite imagery
11 generally show greening trends over Central Asia (Fang et al., 2004; Mohammad et al., 2013).
12 However, in terms of overall water resources management it is important to understand what
13 caused the overall greening (or browning) trend. For example, did it arise because of an
14 expansion (or contraction) of the area being irrigated, or alternatively, the irrigated area might
15 have remained more or less constant and any large scale greening (or browning) trend in
16 vegetation might be related to subtle yet detectable changes in vegetation cover in the
17 extensive deserts in Central Asia. The management implications are quite different for those
18 two scenarios and require a clear separation of these sources of variation.

19 In this paper, we investigate satellite observed (MODIS) vegetation trends (NDVI) in a
20 hyper-arid region of the Heihe River Basin located in northwest China. The aim of this study
21 is to test whether it is possible to separate the vegetation trends in a small relatively well
22 studied basin into components due to climate and due to changes in irrigation. We anticipate
23 that the method might be widely applicable throughout Central Asia.

24 **2 Data and Methods**

25 **2.1 Study Area**

26 We examined part of the landlocked Heihe River Basin in northwest China (40°20'-42°40'N,
27 97°30'-101°45'E) (Fig. 1). Our study area occupies the downstream (northern) part of the
28 basin (Fig. 1b) and is serviced by the regional centre, Ejina, which currently has a population
29 of around 30,000 (<http://www.geohive.com/entry/cn-15.aspx>). The hydro-climate of this
30 predominantly desert environment is extreme. As an indication, at Ejina, the mean annual
31 temperature is around 8°C but day-time excursions in the summer reach 42°C whilst

1 night-time temperatures drop to -36°C during winter (Zhang et al., 2011). The mean annual
2 precipitation over the extensive flatlands is typically less than 50 mm (Fig. 1a) while the mean
3 annual pan evaporation is typically around 3500 mm (Jin et al., 2010; Jia et al., 2011; Wang et
4 al., 2013). Agriculture is only possible via irrigation that is located immediately adjacent to
5 the Heihe River (Fig. 1c). The study area ($\sim 80,000 \text{ km}^2$) is located with the broader Gobi
6 desert and also hosts the second largest area of *Populus euphratica* and *Haloxylon*
7 *ammondendron* forests in China. The basin is generally considered to be the main eco-barrier
8 in northern China (Fu et al., 2007; Qin et al., 2012).

9 The Heihe River (Fig. 1b) is the second longest inland river in China and is the sole river
10 flowing through the Ejina region (Guo et al., 2009). This river originates in the Qilian
11 Mountains. After reaching the mountain outlet at the Yingluoxia hydrological gauge station
12 (Fig.1b), it flows through several oases (Zhangye, Gaotai, Dingxin, Ejina) before terminating
13 at the East and West Juyan Lakes. Zhengyixia station is located downstream of those main
14 oases, where the most water was consumed for agriculture. The discharge at Zhengyixia
15 typically peaks around September each year while the growing season extends from April to
16 October (Fig. 2). Consequently, the irrigated crops in the northern parts of the basin use
17 irrigation water that was discharged from the mountains some 6 months earlier.

18 The river discharge from the mountain regions showed increase trend in past decades.
19 Annual discharge observed at Yingluoxia site increased to $15.7 \times 10^8 \text{ m}^3$ in the 1990s from
20 around $14.4 \times 10^8 \text{ m}^3$ in the 1960s (Fig. 2b). However, the discharge observed at Zhengyixia
21 station located at the place after the river flowing through the oases decreased from around
22 $10.5 \times 10^8 \text{ m}^3$ in the 1960s to around $7.5 \times 10^8 \text{ m}^3$ in the 1990s. The increasing water withdrawal
23 in the upper and middle reaches since the 1960s was associated with increased irrigation (and
24 associated industrial development and urbanization) that made significant reduction in river
25 flows to the downstream oases and accelerated desertification in the northern parts of the
26 basin (Guo et al., 2009; Jin et al., 2010). This phenomenon resulted in the drying-up of East
27 Juyan Lake in 1992 and the drying-up of West Juyan Lake even earlier (Guo et al., 2009).

28 To restore the ecosystem of the downstream Heihe basin the Ecological Water Conveyance
29 Project (EWCP) was launched by the Chinese Government. Water use has been regulated
30 (reduced) since around the year 2000 in the middle parts of the basin thereby delivering more
31 water to the terminal lakes in the northern extremities of the basin (Zhang et al., 2011). In the
32 past decade (2000-2009) the average flow at Zhengyixia has increased to levels (about

1 $10.5 \times 10^8 \text{ m}^3$) not seen since the 1960s (Zhang et al., 2011; Qin et al., 2012). One aim was to
2 reduce degradation of the ecological environment in the northern extremities. Since 2000, an
3 increase in native vegetation growth and species diversity has been attributed to increased
4 groundwater recharge from the increased flows making their way into the northern parts of
5 the basin (Jin et al., 2010; Jia et al., 2011).

6 In summary the basin is a classic source-sink system with water sourced (via snow- and
7 glacier-melt) in the humid mountains in the south that subsequently flows northwards to
8 terminal sinks at the East and West Juyan lakes. With that background we note that many
9 studies have reported trends in vegetation in particular subregions of the basin (Jin et al., 2010;
10 Jia et al., 2011; Wang et al., 2011) but there has yet to be a comprehensive assessment of
11 vegetation trends in the study area. A basin-wide assessment that is useful for hydrologic
12 management requires separation of the overall vegetation trend into a component due to
13 irrigation and a component due to changes in the desert vegetation. That is the aim of the
14 current study.

15 **2.2 MODIS Satellite Observations**

16 Moderate Resolution Imaging Spectroradiometer (MODIS) Terra Vegetation Indices
17 (MOD13Q1) data were acquired from the National Aeronautics and Space Administration
18 (NASA) Earth Observing System Data and Information System (<http://reverb.echo.nasa.gov>)
19 with spatial resolution of 250 m and temporal resolution of 16 days between April 2000 and
20 December 2012. We used the Savitzky-Golay filter (Chen et al., 2004) to minimise noise in
21 the NDVI series prior to further processing. Exploratory analysis highlighted anomalously
22 low NDVI values during many of the winter months that coincided with snow/ice cover. To
23 avoid those anomalous values we restricted the time series to cover the seven month growing
24 season (April-October).

25 **2.3 Identifying the Irrigated Areas**

26 The irrigation regions of interest are restricted to the immediate vicinity of the Heihe River
27 (within the dashed line in Fig. 1c). Within that zone, irrigation is usually supplied by the
28 extraction of groundwater and it is very difficult to distinguish agricultural vegetation from
29 native vegetation that is drawing upon groundwater reserves in the satellite imagery. From the
30 point of view of water resource management, both vegetation types use the same groundwater

1 resources and we made no distinction between them. That enabled us to use a simple
2 threshold approach to identify the vegetated areas of interest because they have much higher
3 green vegetation cover during the April-October growing season.

4 To identify the irrigated area we created a composite image for each year (2000-2012)
5 showing the maximum NDVI recorded during the April-October growing period. We first
6 estimated the mean of the maximum NDVI over adjacent desert regions and found an NDVI
7 of 0.0996 (± 0.024). On that basis we initially defined the irrigated areas as being within the
8 river zone (Fig. 1c) and having an annual maximum NDVI greater than 0.10. To test that
9 threshold we used field surveys showing that irrigated vegetation (that includes native
10 vegetation accessing groundwater) can exist up to a kilometre from the main east river
11 channel in a central part of the basin since the water conveyance project was launched (Guo et
12 al., 2009). We varied the NDVI threshold (0.08, 0.10, 0.12; see Fig. 3) and visually estimated
13 the lateral extent of the vegetation from the river channel. At a threshold of 0.08, the implied
14 irrigation area extended further than 1 km from the main channel while at a threshold of 0.10
15 the extent was some 200-1000 m and close to field survey results (Guo et al., 2009). When the
16 NDVI threshold was set at 0.12, the irrigated area was (incorrectly) shown to be
17 discontinuous (Fig. 3). With that result we were confident that a threshold of 0.10 would
18 correctly identify irrigated areas as defined. That threshold was used to classify the basin land
19 cover into two classes, desert and irrigation, for each year of the period 2000-2012.

20 **2.4 Converting NDVI to Fractional Vegetation Cover**

21 Fractional Vegetation Cover (f_V) was computed from NDVI (V) using a simple linear scaling
22 (Carlson and Ripley, 1997):

$$23 \quad f_V = (V - V_{\min}) / (V_{\max} - V_{\min}) \quad (1)$$

24 where V_{\min} and V_{\max} represent zero green vegetation cover (i.e., bare soil, $f_V = 0$) and complete
25 vegetation cover ($f_V = 1$) respectively. We assume that there are regions of bare soil (e.g.,
26 desert) and of complete vegetation cover (e.g., irrigated agriculture) in the study area of
27 sufficient size relative to the MODIS spatial resolution (250 m) to define the limits of our
28 scaling. To identify those limits we first composited the annual (April-October) maximum V
29 image into a single maximum V image for the entire 13 year (2000-2012) study period. We
30 then conducted a detailed examination of the desert regions and identified an NDVI threshold
31 of 0.05 that was equated to bare ground ($f_V = 0$). To identify the upper limit we investigated

1 small regions of agricultural crops in the maximum composite and identified an NDVI
 2 threshold of 0.65 that was equated to full cover ($f_V = 1$). Those thresholds were used (in Eq. 1)
 3 to re-scale the NDVI data into fractional vegetation cover with values outside the range set to
 4 the respective limits.

5 **2.5 Attribution of Vegetation Changes**

6 With the region split into two land cover types, the regional fractional vegetation cover (f_V)
 7 is determined by fractional vegetation coverage of the irrigated (f_I) and non-irrigated (f_D)
 8 areas and the respective areas (A_I, A_D) for each year,

$$9 \quad f_V = \frac{A_I * f_I + A_D * f_D}{A_I + A_D} \quad (2a)$$

10 Defining the area fractions $A_I^* \left(= \frac{A_I}{A_I + A_D} \right)$ and $A_D^* \left(= \frac{A_D}{A_I + A_D} \right)$ with $A_I^* + A_D^* = 1$, we
 11 rewrite Eq. (2a) as,

$$12 \quad f_V = A_I^* * f_I + A_D^* * f_D \quad (2b)$$

13 The full differential df_V is:

$$14 \quad df_V = \frac{\partial f_V}{\partial f_I} df_I + \frac{\partial f_V}{\partial A_I^*} dA_I^* + \frac{\partial f_V}{\partial f_D} df_D + \frac{\partial f_V}{\partial A_D^*} dA_D^* \\ 15 \quad = A_I^* df_I + f_I dA_I^* + A_D^* df_D + f_D dA_D^* \quad (3)$$

16 The relative change in f_V is given by,

$$17 \quad \frac{df_V}{f_V} = \frac{A_I^* f_I}{f_V} \frac{df_I}{f_I} + \frac{f_I}{f_V} dA_I^* + \frac{A_D^* f_D}{f_V} \frac{df_D}{f_D} + \frac{f_D}{f_V} dA_D^* = X_{fI} + X_{AI} + X_{fD} + X_{AD} \quad (4)$$

18 where the various X terms on the right hand side denote the total change in f_V due to changes
 19 in the greenness (X_{fI}, X_{fD}) and fractional area (X_{AI}, X_{AD}).

20 **2.6 Estimates of Water Availability**

21 The vegetation trends are ultimately compared to estimates of trends in water availability over
 22 the desert and in the irrigation area. We used the monthly discharge gauged at Zhengyixia

1 (Fig. 1b) as a measure of the inflow available for irrigation in Ejina. Over the desert parts of
2 the region, precipitation represents the only input of water. To estimate water availability via
3 precipitation we used three gridded databases ($0.5^\circ \times 0.5^\circ$, monthly, 2000-2010) from the
4 Global Precipitation Climatology Centre (GPCC) (Schneider et al., 2008), Climatic Research
5 Unit (CRU) TS 3.10 (Harris et al., 2013), and the Climate Prediction Center (CPC) (Chen et
6 al., 2002). We also averaged the data from two local meteorological sites (Ejina, Dingxin; see
7 Fig. 1b) as a further check on the gridded databases. Initial analysis showed that precipitation
8 (P) was generally a little higher in the CRU database (but with similar inter-annual variability)
9 while the other two remaining databases gave similar spatial pattern, variability and trend (Fig.
10 4 and Fig. S1). We were most familiar with the GPCC database following previous work (Sun
11 et al., 2012) and subsequently adopted the GPCC database as the precipitation record for the
12 study area (Fig. 4b, c). Note that final interpretations and our conclusions are not sensitive to
13 the choice of precipitation database and we also present the complete analysis using the other
14 spatial databases (CRU, Sites, and CPC) in the supporting material.

15 **3 Results**

16 **3.1 Vegetation Trends**

17 The fractional vegetation cover f_V in this hyper-arid region is very low, with mean growing
18 season f_V of about 3-4%. The oases systems are clearly distinguished by the much higher
19 vegetation cover (Fig. 5a and Fig. S2a). Over the 13 year period (2000-2012) the mean
20 growing season fractional vegetation cover (f_V) showed an increase trend overall, especially in
21 the irrigated oasis (Fig. 5b). So did the annual maximal fractional vegetation cover (Fig. S2).
22 The mean annual fractional vegetation for the whole region increased steadily starting at
23 about 3.2% in 2000 and rising to around to 4.5% in 2012 (Fig. 5c). Fractional vegetation
24 cover in both the desert and irrigated regions also increased and more or less tracked the
25 increase in f_V .

26 The mean growing season fractional vegetation cover in the extensive desert regions (f_D)
27 more or less tracked the changes in the regional total (f_V). The area classified as irrigated only
28 occupies around 3% of total study area with a relatively high growing season average
29 vegetation cover f_I of around 17%. Over the 2000-2012 period, the fractional irrigation area
30 (A_I^*) showed a steady increase (from 3% to 4%) and the mean growing season fractional
31 vegetation cover (f_I) also increased from around 16% to 18%.

1 3.2 Sensitivity Analysis and Trend Attribution

2 3.2.1 Sensitivity

3 After substituting the relevant numerical values ($f_V = 0.039$, $f_I = 0.174$, $A_I^* = 0.033$, $f_D =$
4 0.035 , $A_D^* = 0.967$) derived from the mean growing season (2000-2012) into Eq. (4), the
5 relative change in f_V is,

$$6 \frac{df_V}{f_V} = 0.15 \frac{df_I}{f_I} + 4.45dA_I^* + 0.85 \frac{df_D}{f_D} + 0.88dA_D^* \quad (5)$$

7 The coefficients in equation 5 denote the different sensitivities to change in the overall
8 regional vegetation cover. From that equation we infer that the relative change in fractional
9 green vegetation is most sensitive to variations in the fractional irrigation area (A_I^*). Note that
10 regional vegetation cover is also a factor of around six ($= 0.85/0.15$) times more sensitive to
11 variations in greenness over the desert than over the irrigated regions because the desert land
12 cover type dominates the total area.

13 3.2.2 Trend Attribution

14 From 2000 to 2012, the regional f_V increased by $\sim 25\%$. In terms of the underlying
15 components, the causes of those changes varied from year to year (Fig. 6) but the largest
16 contribution was generally due to changes in f_D (see X_{fD} in Fig. 6) with a smaller contribution
17 due to changes in A_I^* (X_{AI} in Fig. 6). Variations in the remaining terms (X_{fI} , X_{AD}) had little
18 impact on trends in the overall regional vegetation cover.

19 3.2.3 Uncertainty Analysis

20 The major source of uncertainty in our results relates to the NDVI threshold used to
21 distinguish the irrigated and desert regions (Section 2.3, Fig. 3). To evaluate the robustness of
22 our results we also calculated the relative change in fractional vegetation cover using five
23 different NDVI thresholds (0.08, 0.09, 0.10, 0.11, 0.12; Table 1). Those results show that
24 while the numerical value of the sensitivity coefficients does change, the overall conclusion
25 that regional vegetation cover is most sensitive to changes in irrigation area remains
26 unchanged. Similarly, the attribution results for different thresholds show that most of the
27 change in regional vegetation cover remained due to changes in desert greenness and in the
28 area of irrigation.

1 3.3 Predicting Regional Vegetation Cover Based on Water Availability

2 The earlier results (Sections 3.2.2, 3.2.3) show that the regional vegetation cover trend mainly
3 depends on fractional vegetation cover over the extensive desert regions and the area of the
4 irrigated lands. With that result, we approximate Eq. (4) as,

$$5 \frac{df_V}{f_V} \sim \frac{f_I}{f_V} dA_I^* + \frac{A_D^*}{f_V} df_D \quad (6)$$

6 In this region the area of land irrigated each year is dependent on the inflow at an earlier time
7 while greenness in the desert areas is dependent on precipitation. To test that we use the 12
8 month GPCP precipitation estimate to the end of the growing season (previous
9 November-October) to estimate the growing season desert vegetation cover. The results show
10 a positive relationship ($p < 0.05$, Fig. 7) and imply that the desert vegetation cover increases by
11 0.017% for each additional mm of annual P . (The analysis based on other precipitation
12 databases (CRU, Sites, and CPC) is included in the supporting materials (Fig. S3 and Table
13 S1).

14 We sought a similar predictive relation between the total runoff (R) in the previous calendar
15 year at Zhengyixia and the fractional irrigated area (A_I^*) (Fig. 8). The results reveal a strong
16 positive relationship ($p = 0.002$) where an increase in inflow at Zhengyixia of $1 \times 10^8 \text{ m}^3$ will
17 increase the fractional area of irrigation by around 0.1%.

18 The results allow us to modify the earlier expression by replacing dA_I^* with αdR (Fig. 8)
19 and df_D with βdP (Fig. 7) respectively,

$$20 \frac{df_V}{f_V} \sim \frac{f_I}{f_V} \alpha dR + \frac{A_D^*}{f_V} \beta dP \quad (7)$$

21 Expressing that in a relative form we have,

$$22 \frac{df_V}{f_V} \sim \frac{f_I}{f_V} \alpha R \frac{dR}{R} + \frac{A_D^*}{f_V} \beta P \frac{dP}{P}$$

23 Taking the long term mean annual values ($f_I = 0.17$, $f_V = 0.038$, $R = 9.67$, $P = 47.5$, $A_D^* = 0.97$)
24 and the empirical coefficients ($\alpha = 0.0011$, Fig. 8; $\beta = 0.00017$, Fig. 7) we have,

$$25 \frac{df_V}{f_V} \sim 0.05 \frac{dR}{R} + 0.21 \frac{dP}{P} = X_R + X_P \quad (8)$$

1 The empirically based equation predicts that a 1% variation in runoff would leads to a 0.05%
2 variation in f_V whilst a 1% variation in precipitation would increase f_V by 0.21%. Finally we
3 use the runoff and precipitation data to estimate the relative changes in regional vegetation
4 cover. The overall result shows that the model developed here accounts for *c.* 52% of the total
5 variance in regional vegetation cover (Fig. 9). It varied from 45%-62% depending on different
6 precipitation databases (Fig. S4).

7 **4 Discussions**

8 In this study, we focused on a hyper-arid oasis-desert system where agricultural crops
9 (artificial oasis) and groundwater-fed native vegetation (natural oasis) that occupy some 4%
10 of the entire region are concentrated along the Heihe River. As is well known, it is very hard
11 to evaluate sparse desert vegetation cover in hyper-arid regions at a regional scale owing to
12 coarse spatial and spectral resolution (Fensholt and Proud, 2012). However, the high
13 resolution The MODIS sensor has spectral bands that are specifically designed for vegetation
14 monitoring and MODIS-based vegetation indices are known to perform well in discriminating
15 vegetation differences in both sparsely, and densely, vegetated areas (Huete et al., 2002).
16 Therefore, a vegetation index from MODIS with 250m spatial resolution is likely to be
17 appropriate for monitoring of fragmented landscapes of drylands, e.g. Central Asia (Dubovyk
18 et al., 2013) and provides a potentially useful data source to evaluate regional vegetation
19 change.

20 We found it necessary to restrict our analysis to the growing season to avoid noise
21 apparently caused by snow and ice. With that pre-processing, our results showed that the
22 mean growing season fractional vegetation cover (f_V) in Ejina showed a steady increase from
23 $\sim 3.2\%$ in 2000 and rising to $\sim 4.5\%$ in 2012. The key question is what caused this change;
24 the general climate variability or human-induced land use changes relating to irrigation?

25 We were able to identify the crops and green native vegetation along the river using the
26 elevated NDVI signal during the April-October growing season but we were unable to
27 separate the crops from the native vegetation using the MODIS NDVI satellite data. With that,
28 the entire region was split into two land cover types, denoted here as desert and irrigation
29 oasis (that includes native vegetation along the river) for each year. Desert is distinguished
30 from irrigated lands using a simple maximal NDVI threshold (Fig. 3).

31 Regional vegetation cover depends on both the desert and irrigated vegetation cover
32 and their area fractions. Regional vegetation cover in the downstream of the Heihe River

1 Basin (2000-2012) is highly sensitive to variations in the area of irrigated land (Eq. 5).
2 Over the whole period we found that the contributions to regional vegetation cover change
3 due to changes in irrigated vegetation cover (f_I) and the area fraction (A_I^*) were 7.8% and
4 20.5% respectively, whilst changes in the non-irrigated vegetation cover (f_D) and area
5 fraction (A_D^*) accounted for 75.8%, and -4.1% respectively. Uncertainty analysis indicated
6 that the fractional changes were not especially sensitive to the assumed NDVI threshold
7 that was used to delineate desert from irrigated lands (Table 1). With that, our final result
8 was that the relative vegetation change over the basin was most sensitive to changes in
9 greenness of desert vegetation (~75%, Table 1) and in the area of irrigation (~21%, Table
10 1). The remaining terms (greenness of irrigated vegetation, area of desert) could be ignored.

11 To be able to prognostically estimate changes in relative vegetation cover we sought
12 empirical relations between desert greenness and precipitation (Fig. 7) and between the extent
13 of irrigation and runoff in the previous year (Fig. 8). Gridded databases supplied a useful way
14 to estimate the precipitation and its spatial distribution. Therefore, as expected, vegetation
15 cover in the non-irrigated f_D was strongly related to scarcity, discrete annual precipitation in
16 such an arid region (Fig. 6) (Bhuiyan, 2008; D'Odorico and Porporato, 2006). The underlying
17 basis of that latter relation would be complex and would involve a lag because (i) farmers
18 may anticipate future planting areas based on runoff from the previous year/s, and (ii) the
19 runoff recharges the local groundwater that is subsequently used by the local population (for
20 irrigation) and by the native oasis vegetation. The lagged relation between runoff and the area
21 of irrigation may provide a useful empirical basis for forecasting and confirms the importance
22 of managing the human impact to achieve targeted improvements in the regional ecology. For
23 the lower reaches, that empirical relation can be used to estimate water use based on the
24 previous runoff.

25 It is difficult to discriminate the effects of climate change and of human activities on
26 regional vegetation change in arid regions (Zhou et al., 2013). In northwest China, previous
27 work has suggested that precipitation is the most important factor (Ma and Frank, 2006) while
28 other studies concluded that climate factors only played a small role with the major cause of
29 regional vegetation change being caused agricultural activities (Kong et al., 2010; Zhou et al.,
30 2013). The results varied with time and space. Most of the studies are limited to qualitative
31 distinctions (Dai et al., 2011), model estimation (Zhang et al., 2011; Zhou et al., 2013), and
32 regression and residual approximation (Wang et al., 2012). To resolve those differences we

1 used a formal analytic framework to attribute the change of regional vegetation cover. The
2 separation and attribution between extensive desert regions and irrigation area supplied a
3 useful way to quantify the vegetation contributions from land use changes relating to
4 irrigation and climate variability.

5 The reason why we can use this method in this ecologically delicate and highly concerned
6 area is that the most human activities focus on the irrigated oasis that accounts for 3% - 5% of
7 the total area. It is a typical oasis-desert landscape that dominates Central Asia with
8 widespread irrigation oases. In this system, the allocation of water resources is critical in
9 achieving a balance among different oases as well as between human water appropriation for
10 irrigation and ecological conservation. The overuse water in the upper and middle reaches
11 associated with increased irrigation made significant reduction in river flows to the
12 downstream oases and accelerated desertification. A similar over use of water for irrigation
13 also happened in the Aral Sea. The water withdrawal for agricultural expansion (e.g. from
14 about 4.5 Mha in 1960 to almost 7.9 Mha by 1999) led to a dramatic shrinkage of the Aral
15 Sea that has attracted the attention of the international scientific community over the last few
16 decades (Micklin, 1988; Whish-Wilson, 2002; Lioubimtseva et al., 2005). In the last few
17 decades, the runoff from mountains showed an increase trend with more precipitation and
18 warmer climate (Unger-Shayesteh et al., 2013; Wang et al., 2013). However, rational
19 distribution and sustainable management of water resources is still a long-term and arduous
20 task. Our results suggest that it is possible to use remotely sensed data to provide practical
21 support in assessing the ecological status of irrigation regions that surround most Central
22 Asian rivers.

23 **5 Conclusions**

24 We found that the regional fractional vegetation cover f_V in the downstream parts of the
25 greater Heihe River basin increased by 25% from 2000 to 2012. The largest contribution was
26 due to a slight greening of the desert regions that was consistent with increased precipitation
27 over the period. The other main contribution to the regional trend was an expansion of
28 irrigated areas (including native vegetation dependent on groundwater) along the Heihe River
29 that was found to be dependent on the runoff in the previous year. In conclusion, water
30 availability both from precipitation and runoff can explain around 52% of the total variance in
31 regional vegetation cover over the period in this extremely arid environment. This study
32 showed that it is feasible to separate the variations in regional vegetation cover that are due to

1 changes in the climate from those due to changes in human activities given appropriate
2 regional context.

3 **Acknowledgements**

4 This study was supported by the National Program on Key Basic Research Project of China
5 (2010CB951003) and China Scholarship Council. Vegetation type data set is provided by
6 Environmental and Ecological Science Data Center for West China, National Natural Science
7 Foundation of China (<http://westdc.westgis.ac.cn>). We thank three anonymous reviewers for
8 their insightful comments and suggestions that improved this manuscript.

9

1 **References**

- 2 Angelini, I. M., Garstang, M., Davis, R. E., Hayden, B., Fitzjarrald, D. R., Legates, D. R.,
3 Greco, S., Macko, S., and Connors, V.: On the coupling between vegetation and the
4 atmosphere, *Theor. Appl. Climatol.*, 105, 243-261, doi: 10.1007/s00704-010-0377-5, 2011.
- 5 Bhuiyan, C.: Desert vegetation during droughts: response and sensitivity, *The International*
6 *Archives of the Photogrammetry, Remote Sensing and Spatial Information Sciences*, 37,
7 907-912, 2008.
- 8 Bonan, G. B., Levis, S., Sitch, S., Vertenstein, M., and Oleson, K. W.: A dynamic global
9 vegetation model for use with climate models: concepts and description of simulated
10 vegetation dynamics, *Global Change Biol.*, 9, 1543-1566, doi:
11 10.1046/j.1365-2486.2003.00681.x, 2003.
- 12 Bond, W., Midgley, G., and Woodward, F.: The importance of low atmospheric CO₂ and fire
13 in promoting the spread of grasslands and savannas, *Global Change Biol.*, 9, 973-982, doi:
14 10.1046/j.1365-2486.2003.00577.x, 2003.
- 15 Bounoua, L., Hall, F. G., Sellers, P. J., Kumar, A., Collatz, G. J., Tucker, C. J., and Imhoff, M.
16 L.: Quantifying the negative feedback of vegetation to greenhouse warming: A modeling
17 approach, *Geophys. Res. Lett.*, 37, doi: 10.1029/2010gl045338, 2010.
- 18 Box, E. O., Holben, B. N., and Kalb, V.: Accuracy of the Avhrr Vegetation Index as a
19 Predictor of Biomass, Primary Productivity and Net CO₂ Flux, *Vegetatio*, 80, 71-89, doi:
20 10.1007/Bf00048034, 1989.
- 21 Carlson, T. N., and Ripley, D. A.: On the relation between NDVI, fractional vegetation cover,
22 and leaf area index, *Remote Sens. Environ.*, 62, 241-252, doi:
23 10.1016/S0034-4257(97)00104-1, 1997.
- 24 Chen, J., Jonsson, P., Tamura, M., Gu, Z. H., Matsushita, B., and Eklundh, L.: A simple
25 method for reconstructing a high-quality NDVI time-series data set based on the
26 Savitzky-Golay filter, *Remote Sens. Environ.*, 91, 332-344, doi: 10.1016/j.rse.2004.03.014,
27 2004.
- 28 Chen, M. Y., Xie, P. P., Janowiak, J. E., and Arkin, P. A.: Global land precipitation: A 50-yr
29 monthly analysis based on gauge observations, *J. Hydrometeorol.*, 3, 249-266, doi:
30 10.1175/1525-7541(2002)003<0249:Glpaym>2.0.Co;2, 2002.
- 31 Dai, S. P., Zhang, B., Wang, H. J., Wang, Y. M., Guo, L. X., Wang, X. M., and Li, D.:
32 Vegetation cover change and the driving factors over northwest China, *J. Arid Land*, 3, 25-33,
33 10.3724/sp.j.1227.2011.00025, 2011.
- 34 Dirnböck, T., Grandin, U., Bernhardt - Römermann, M., Beudert, B., Canullo, R., Forsius, M.,
35 Grabner, M. T., Holmberg, M., Kleemola, S., and Lundin, L.: Forest floor vegetation response
36 to nitrogen deposition in Europe, *Global Change Biol.*, 20, 429-440, doi: 10.1111/gcb.12440,
37 2014.
- 38 Donohue, R. J., McVicar, T. R., and Roderick, M. L.: Climate-related trends in Australian
39 vegetation cover as inferred from satellite observations, 1981-2006, *Global Change Biol.*, 15,
40 1025-1039, doi: 10.1111/j.1365-2486.2008.01746.x, 2009.

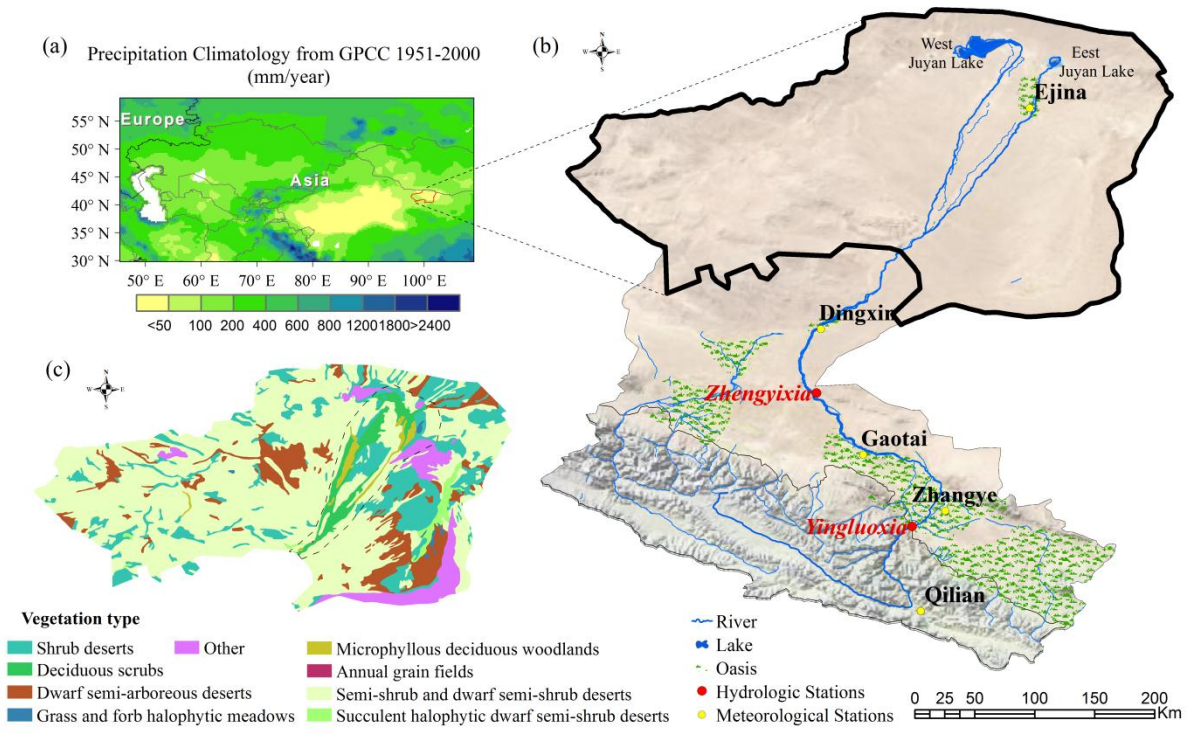
- 1 Donohue, R. J., Roderick, M. L., McVicar, T. R., and Farquhar, G. D.: Impact of CO₂
2 fertilization on maximum foliage cover across the globe's warm, arid environments, *Geophys.*
3 *Res. Lett.*, 40, 3031-3035, doi: 10.1002/grl.50563, 2013.
- 4 D'Odorico, P., and Porporato, A.: *Dryland ecohydrology*, Springer, 2006.
- 5 Dubovyk, O., Menz, G., Conrad, C., Kan, E., Machwitz, M., and Khamzina, A.:
6 Spatio-temporal analyses of cropland degradation in the irrigated lowlands of Uzbekistan
7 using remote-sensing and logistic regression modeling, *Environ. Monit. Assess.*, 185,
8 4775-4790, doi: 10.1007/s10661-012-2904-6, 2013.
- 9 Fang, J. Y., Piao, S. L., He, J. S., and Ma, W. H.: Increasing terrestrial vegetation activity in
10 China, 1982-1999, *Sci. China Ser. C*, 47, 229-240, doi: 10.1360/03yc0068, 2004.
- 11 Fensholt, R., and Proud, S. R.: Evaluation of earth observation based global long term
12 vegetation trends—Comparing GIMMS and MODIS global NDVI time series, *Remote Sens.*
13 *Environ.*, 119, 131-147, doi:10.1016/j.rse.2011.12.015, 2012.
- 14 Fensholt, R., Rasmussen, K., Kaspersen, P., Huber, S., Horion, S., and Swinnen, E.:
15 Assessing Land Degradation/Recovery in the African Sahel from Long-Term Earth
16 Observation Based Primary Productivity and Precipitation Relationships, *Remote Sens.*, 5,
17 664-686, doi: 10.3390/Rs5020664, 2013.
- 18 Fu, K., Chen, X. P., Liu, Q. G., and Li, C. H.: Land use and land cover changes based on
19 remote sensing and GIS in Heihe River basin, China, *IEEE International Symposium on*
20 *Geoscience and Remote Sensing*, 1790-1793, 2007.
- 21 Gerten, D., Schaphoff, S., Haberlandt, U., Lucht, W., and Sitch, S.: Terrestrial vegetation and
22 water balance - hydrological evaluation of a dynamic global vegetation model, *J. Hydrol.*, 286,
23 249-270, doi: 10.1016/j.jhydrol.2003.09.029, 2004.
- 24 Goetz, S. J., Bunn, A. G., Fiske, G. J., and Houghton, R.: Satellite-observed photosynthetic
25 trends across boreal North America associated with climate and fire disturbance, *Proc. Natl.*
26 *Acad. Sci. USA*, 102, 13521-13525, doi:10.1073/pnas.0506179102, 2005.
- 27 Guo, Q. L., Feng, Q., and Li, J. L.: Environmental changes after ecological water conveyance
28 in the lower reaches of Heihe River, northwest China, *Environ. Geol.*, 58, 1387-1396, doi:
29 10.1007/s00254-008-1641-1, 2009.
- 30 Harris, I., Jones, P., Osborn, T., and Lister, D.: Updated high - resolution grids of monthly
31 climatic observations - the CRU TS3. 10 Dataset, *Int. J. Climatol.*, 34, 623-642, doi:
32 10.1002/joc.3711, 2013.
- 33 Herrmann, S. M., Anyamba, A., and Tucker, C. J.: Recent trends in vegetation dynamics in
34 the African Sahel and their relationship to climate, *Global Environ. Chang.*, 15, 394-404, doi:
35 10.1016/j.gloenvcha.2005.08.004, 2005.
- 36 Huete, A., Didan, K., Miura, T., Rodriguez, E. P., Gao, X., and Ferreira, L. G.: Overview of
37 the radiometric and biophysical performance of the MODIS vegetation indices, *Remote Sens.*
38 *Environ.*, 83, 195-213, doi: 10.1016/S0034-4257(02)00096-2, 2002.
- 39 Hutchinson, C. F., Unruh, J. D., and Bahre, C. J.: Land use vs. climate as causes of vegetation
40 change: a study in SE Arizona, *Global Environ. Chang.*, 10, 47-55, doi:
41 10.1016/S0959-3780(00)00009-1, 2000.

- 1 Jia, L., Shang, H., Hu, G., and Menenti, M.: Phenological response of vegetation to upstream
2 river flow in the Heihe Rive basin by time series analysis of MODIS data, *Hydrol. Earth. Syst.*
3 *Sci.*, 15, 1047-1064, doi: 10.5194/hess-15-1047-2011, 2011.
- 4 Jin, X. M., Schaepman, M., Clevers, J., Su, Z. B., and Hu, G. C.: Correlation Between Annual
5 Runoff in the Heihe River to the Vegetation Cover in the Ejina Oasis (China), *Arid Land Res.*
6 *Manag.*, 24, 31-41, doi: 10.1080/15324980903439297, 2010.
- 7 Kong, W., Sun, O., Chen, Y., Yu, Y., and Tian, Z.: Patch-level based vegetation change and
8 environmental drivers in Tarim River drainage area of West China, *Landscape Ecol.*, 25,
9 1447-1455, 10.1007/s10980-010-9505-y, 2010.
- 10 Lim, C., Kafatos, M., and Megonigal, P.: Correlation between atmospheric CO2
11 concentration and vegetation greenness in North America: CO2 fertilization effect, *Climate*
12 *Res.*, 28, 11-22, doi: 10.3354/cr028011, 2004.
- 13 Lioubimtseva, E., Cole, R., Adams, J. M., and Kapustin, G.: Impacts of climate and
14 land-cover changes in arid lands of Central Asia, *J. Arid Environ.*, 62, 285-308, doi:
15 10.1016/j.jaridenv.2004.11.005, 2005.
- 16 Lioubimtseva, E., and Henebry, G. M.: Climate and environmental change in arid Central
17 Asia: Impacts, vulnerability, and adaptations, *J. Arid Environ.*, 73, 963-977, doi:
18 10.1016/j.jaridenv.2009.04.022, 2009.
- 19 Ma, M., and Frank, V.: Interannual variability of vegetation cover in the Chinese Heihe River
20 Basin and its relation to meteorological parameters, *Int. J. Remote Sens.*, 27, 3473-3486,
21 10.1080/01431160600593031, 2006.
- 22 Micklin, P. P.: Desiccation of the Aral Sea - a Water Management Disaster in the
23 Soviet-Union, *Science*, 241, 1170-1175, doi: 10.1126/science.241.4870.1170, 1988.
- 24 Mohammat, A., Wang, X. H., Xu, X. T., Peng, L. Q., Yang, Y., Zhang, X. P., Myneni, R. B.,
25 and Piao, S. L.: Drought and spring cooling induced recent decrease in vegetation growth in
26 Inner Asia, *Agr. Forest. Meteorol.*, 178, 21-30, doi: 10.1016/j.agrformet.2012.09.014, 2013.
- 27 Myneni, R. B., Keeling, C. D., Tucker, C. J., Asrar, G., and Nemani, R. R.: Increased plant
28 growth in the northern high latitudes from 1981 to 1991, *Nature*, 386, 698-702, doi:
29 10.1038/386698a0, 1997.
- 30 Nemani, R. R., Keeling, C. D., Hashimoto, H., Jolly, W. M., Piper, S. C., Tucker, C. J.,
31 Myneni, R. B., and Running, S. W.: Climate-driven increases in global terrestrial net primary
32 production from 1982 to 1999, *Science*, 300, 1560-1563, doi: 10.1126/science.1082750, 2003.
- 33 Pielke, R. A., Avissar, R., Raupach, M., Dolman, A. J., Zeng, X. B., and Denning, A. S.:
34 Interactions between the atmosphere and terrestrial ecosystems: influence on weather and
35 climate, *Global Change Biol.*, 4, 461-475, doi: 10.1046/j.1365-2486.1998.t01-1-00176.x,
36 1998.
- 37 Qin, D. J., Zhao, Z. F., Han, L. F., Qian, Y. P., Ou, L., Wu, Z. Q., and Wang, M. C.:
38 Determination of groundwater recharge regime and flowpath in the Lower Heihe River basin
39 in an arid area of Northwest China by using environmental tracers: Implications for
40 vegetation degradation in the Ejina Oasis, *Appl. Geochem.*, 27, 1133-1145, doi:
41 10.1016/j.apgeochem.2012.02.031, 2012.
- 42 Rahimov, S.: Impacts of climate change on water resources in Central Asia, *Documentos*
43 *CIDOB. Asia*, 33-56, 2009.

- 1 Schneider, U., Fuchs, T., Meyer-Christoffer, A., and Rudolf, B.: Global precipitation analysis
2 products of the GPCC, Global Precipitation Climatology Centre (GPCC), DWD, Internet
3 Publikation, 1-12, 2008.
- 4 Sun, F. B., Roderick, M. L., and Farquhar, G. D.: Changes in the variability of global land
5 precipitation, *Geophys Res. Lett.*, 39, doi: 10.1029/2012gl053369, 2012.
- 6 Thonicke, K., Venevsky, S., Sitch, S., and Cramer, W.: The role of fire disturbance for global
7 vegetation dynamics: coupling fire into a Dynamic Global Vegetation Model, *Global Ecol.*
8 *Biogeogr.*, 10, 661-677, 2001.
- 9 Tucker, C. J.: Red and Photographic Infrared Linear Combinations for Monitoring Vegetation,
10 *Remote Sens. Environ.*, 8, 127-150, doi: 10.1016/0034-4257(79)90013-0, 1979.
- 11 Unger-Shayesteh, K., Vorogushyn, S., Farinotti, D., Gafurov, A., Duethmann, D., Mandychhev,
12 A., and Merz, B.: What do we know about past changes in the water cycle of Central Asian
13 headwaters? A review, *Global Planet. Change*, 110, Part A, 4-25, doi:
14 10.1016/j.gloplacha.2013.02.004, 2013.
- 15 Wang, P., Zhang, Y. C., Yu, J. J., Fu, G. B., and Ao, F.: Vegetation dynamics induced by
16 groundwater fluctuations in the lower Heihe River Basin, northwestern China, *J. Plant*
17 *Ecol-UK*, 4, 77-90, doi: 10.1093/Jpe/Rtr002, 2011.
- 18 Wang, T., Sun, J. G., Han, H., and Yan, C. Z.: The relative role of climate change and human
19 activities in the desertification process in Yulin region of northwest China, *Environ. Monit.*
20 *Assess.*, 184, 7165-7173, 10.1007/s10661-011-2488-6, 2012.
- 21 Wang, Y., Shen, Y., Chen, Y., and Guo, Y.: Vegetation dynamics and their response to
22 hydroclimatic factors in the Tarim River Basin, China, *Ecohydrology*, 6, 927-936,
23 10.1002/eco.1255, 2013.
- 24 Wang, Y., Feng, Q., Chen, L. J., and Yu, T. F.: Significance and Effect of Ecological
25 Rehabilitation Project in Inland River Basins in Northwest China, *Environ. Manage.*, 52,
26 209-220, doi: 10.1007/s00267-013-0077-x, 2013.
- 27 Whish-Wilson, P.: The Aral Sea environmental health crisis, *Journal of Rural and Remote*
28 *Environmental Health*, 1, 29-34, 2002.
- 29 Yao, T. D., Wang, Y. Q., Liu, S. Y., Pu, J. C., Shen, Y. P., and Lu, A. X.: Recent glacial
30 retreat in High Asia in China and its impact on water resource in Northwest China, *Sci. China*
31 *Ser. D*, 47, 1065-1075, doi: 10.1360/03yd0256, 2004.
- 32 Yu, J., and Wang, P.: Relationship between Water and Vegetation in the Ejina Delta, *Bulletin*
33 *of the Chinese Academy of Sciences*, 26, 68-75, 2012.
- 34 Zhang, C. X., Wang, X. M., Li, J. C., and Hua, T.: Roles of climate changes and human
35 interventions in land degradation: a case study by net primary productivity analysis in China's
36 Shiyanghe Basin, *Environ. Earth Sci.*, 64, 2183-2193, 10.1007/s12665-011-1046-4, 2011.
- 37 Zhang, Y. C., Yu, J. J., Wang, P., and Fu, G. B.: Vegetation responses to integrated water
38 management in the Ejina basin, northwest China, *Hydrol. Process.*, 25, 3448-3461, doi:
39 10.1002/Hyp.8073, 2011.
- 40 Zhao, C., Li, S., Feng, Z., and Shen, W.: Dynamics of groundwater level in the water table
41 fluctuant belt at the lower reaches of Heihe River, *Journal of Desert Research*, 29, 365-370,
42 2009.

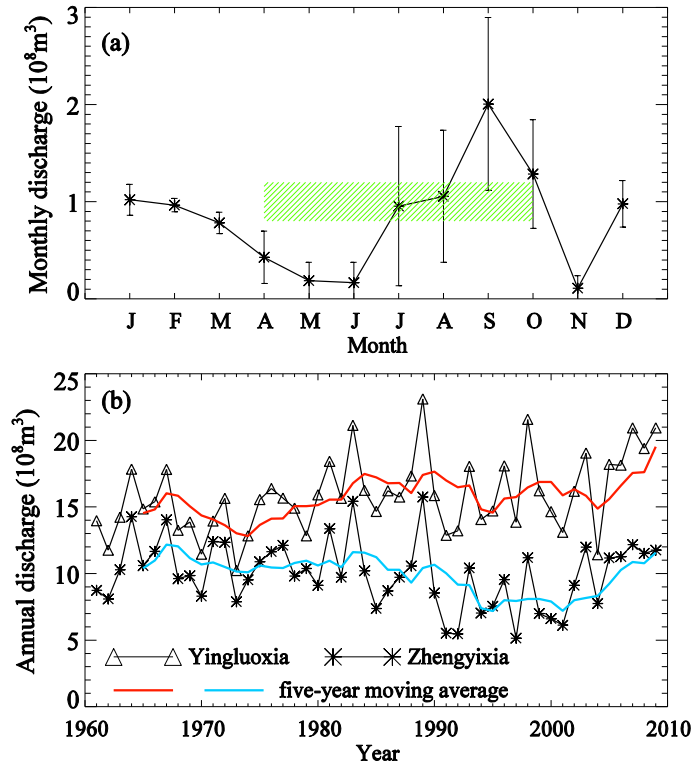
1 Zhou, W., Sun, Z., Li, J., Gang, C., and Zhang, C.: Desertification dynamic and the relative
 2 roles of climate change and human activities in desertification in the Heihe River Basin based
 3 on NPP, *J. Arid Land*, 5, 465-479, 10.1007/s40333-013-0181-z, 2013.

4
 5

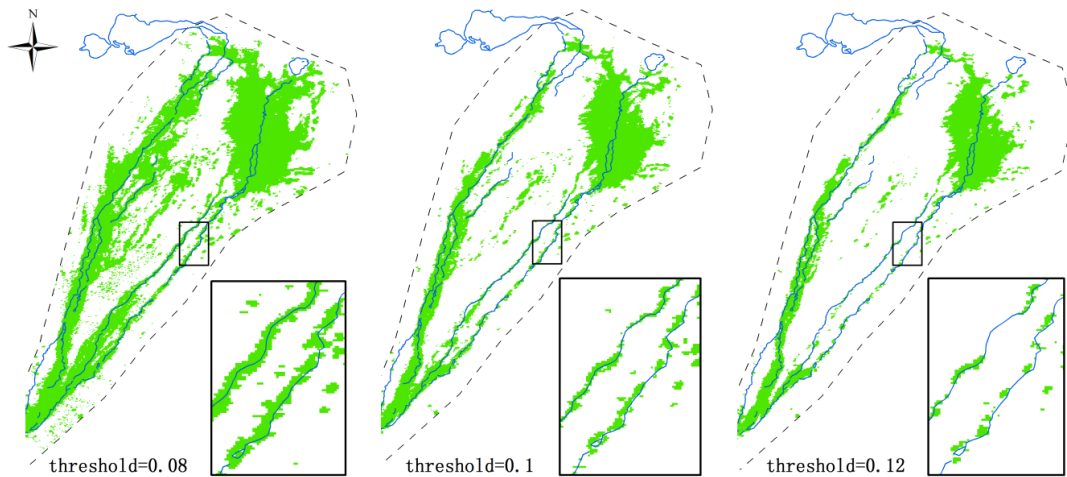


6
 7
 8
 9

Fig. 1 Details of the study area. (a) Regional setting and the mean annual precipitation (1951-2000). (b) Landscape of Heihe River Basin with location of meteorological and hydrologic observation sites. (c) Vegetation Map of lower Heihe river basin where the dashed line denotes the bounds of the possible irrigation area.

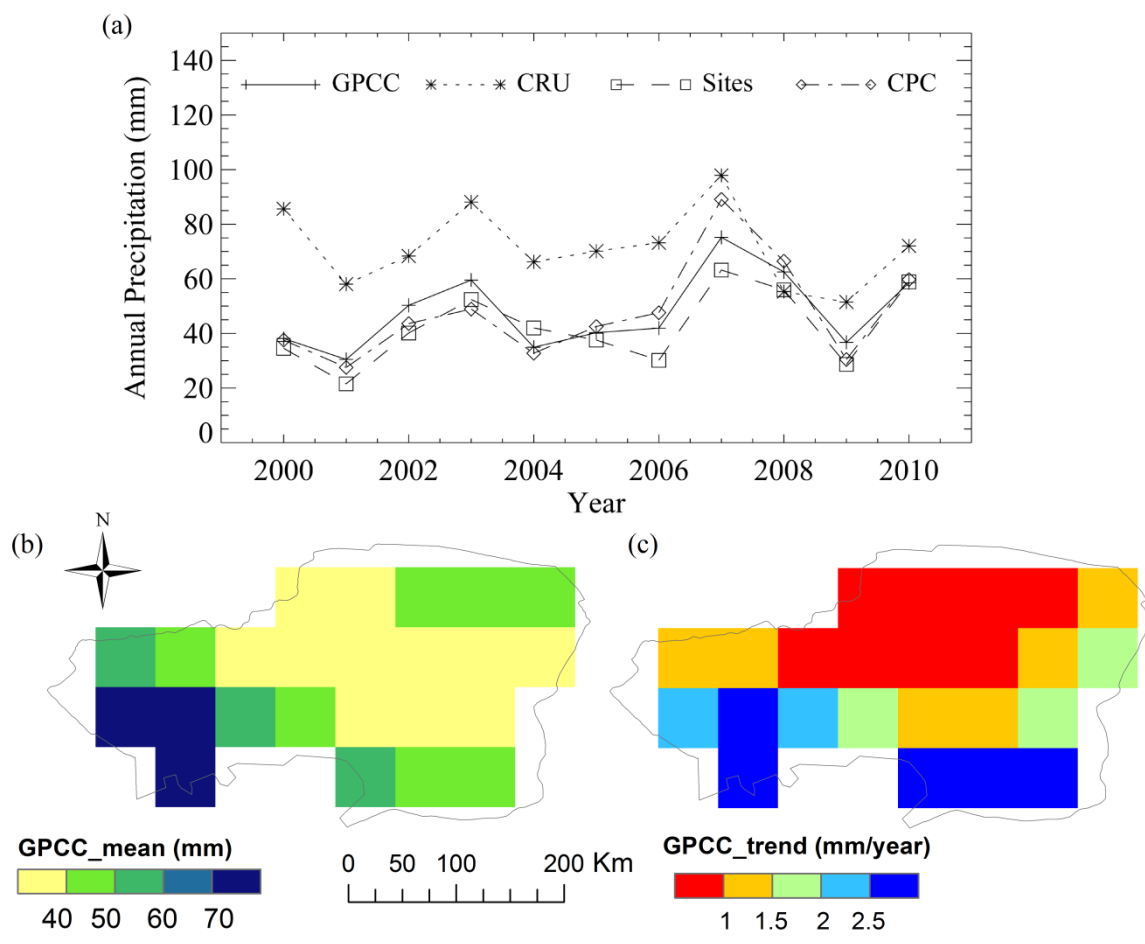


1
 2 Fig. 2 River flows in the Heihe River basin. (a) Mean monthly river discharge (bars indicate standard deviation)
 3 of Heihe River (2000-2009) at Zhengyixia station in relation to the growing season (diagonal stripes). (b) Annual
 4 discharge of Heihe River (1961-2009) at Yingluoxia and Zhengyixia stations

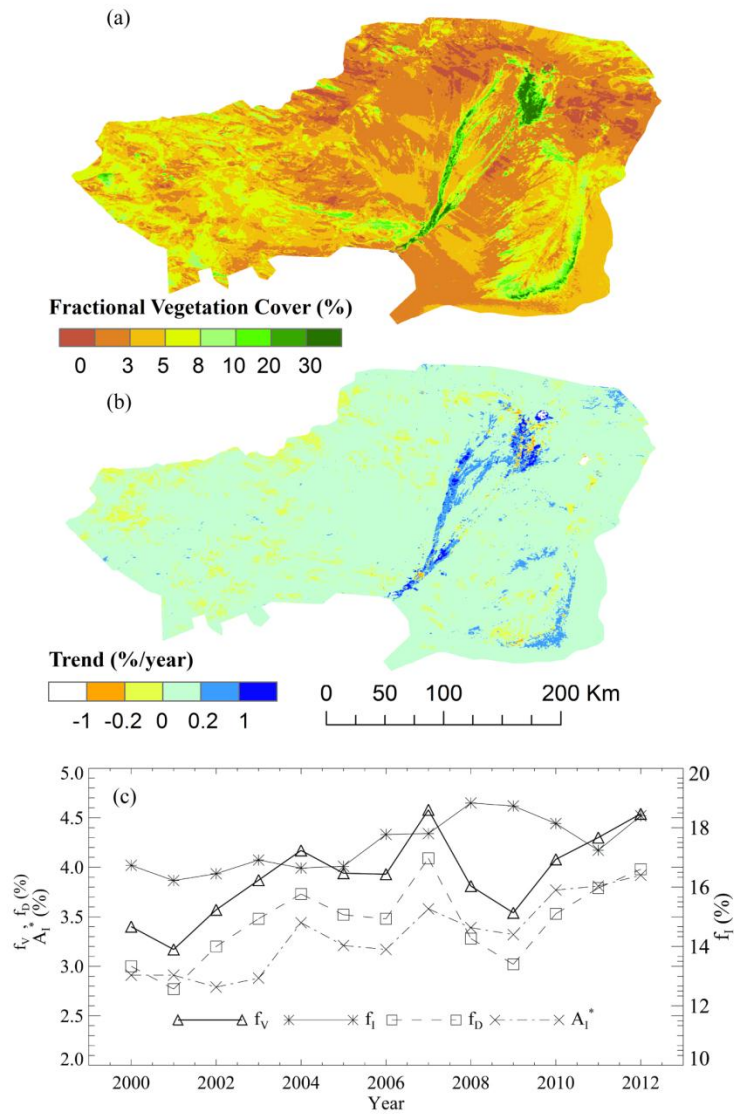


6
 7 Fig. 3 Irrigated areas derived using different NDVI thresholds

8

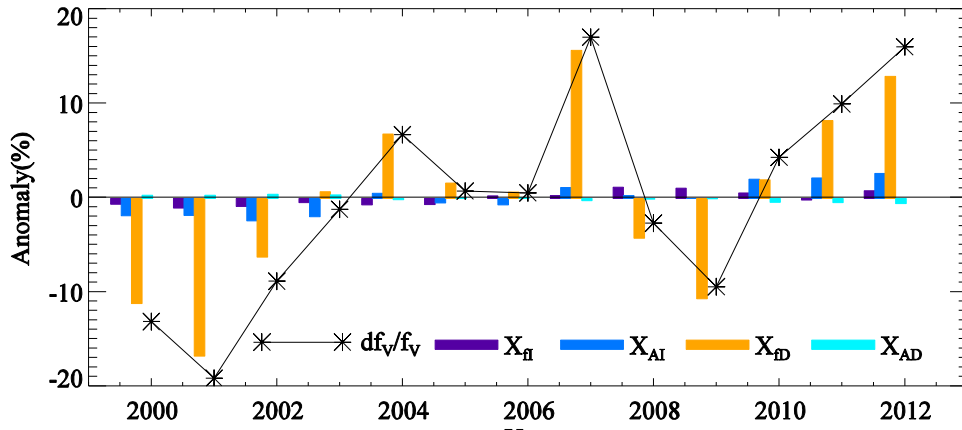


1
 2 Fig. 4 Spatial-temporal change of precipitation for the study area. (a) Annual precipitation per four different data
 3 sources (as indicated); (b) Mean annual precipitation from GPCCC, and (c) the trend from 2000 to 2010.



1
2
3
4
5
6
7

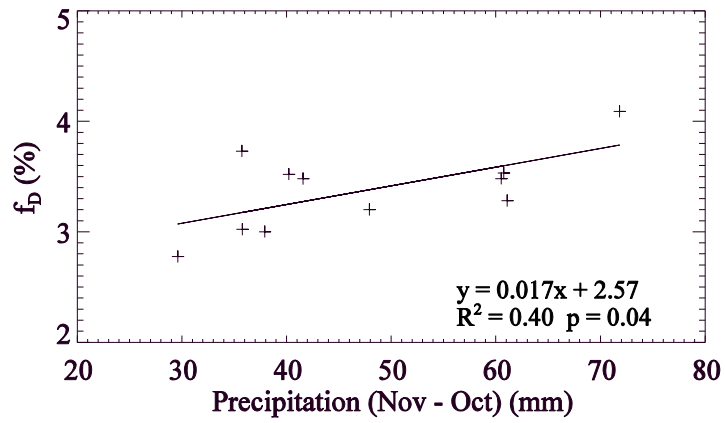
Fig. 5 Spatial-temporal change of the growing season (April-October) mean annual fractional vegetation cover (2000-2012). (a) Spatial pattern of growing season (April-October) mean annual fractional vegetation cover; (b) Spatial trend of growing season (April-October) mean annual fractional vegetation cover (2000-2012); (c) Trends in the growing season (April-October) mean annual fractional vegetation for the whole region (f_v , left scale), desert (f_D , left scale) and irrigated (f_I , right scale) land cover classes, and for the fractional area of irrigation (A_I^* , left scale).



1
2 Fig.6 Annual changes in relative vegetation cover (df_v/f_v) and the underlying components from mean annual
3 fractional vegetation for the desert (X_{fD}) and for the irrigated (X_{fI}) regions along with changes in
4 the fractional area of desert (X_{AD}) and irrigated (X_{AI}) regions.

5
6 Table 1 Sensitivity and attribution uncertainty with varied NDVI thresholds to define irrigated and
7 non-irrigated region (mean annual fractional vegetation for the whole region f_v , irrigated oasis f_I and desert
8 f_D , fractional area of irrigation A_I^* and desert A_D^* ; And their attribution X_{fI} , X_{AI} , X_{fD} , X_{AD})

NDVI Threshold	Sensitivity	Attribution			
		X_{fI}	X_{AI}	X_{fD}	X_{AD}
0.08	$\frac{df_v}{f_v} = 0.18 \frac{df_I}{f_I} + 2.97dA_I^* + 0.82 \frac{df_D}{f_D} + 0.88dA_D^*$	14.0%	16.8%	74.1%	-5.0%
0.09	$\frac{df_v}{f_v} = 0.16 \frac{df_I}{f_I} + 3.76dA_I^* + 0.84 \frac{df_D}{f_D} + 0.88dA_D^*$	9.5%	19.4%	75.6%	-4.5%
0.1	$\frac{df_v}{f_v} = 0.15 \frac{df_I}{f_I} + 4.45dA_I^* + 0.85 \frac{df_D}{f_D} + 0.88dA_D^*$	7.8%	20.5%	75.8%	-4.1%
0.11	$\frac{df_v}{f_v} = 0.14 \frac{df_I}{f_I} + 4.99dA_I^* + 0.86 \frac{df_D}{f_D} + 0.89dA_D^*$	7.6%	20.3%	75.7%	-3.6%
0.12	$\frac{df_v}{f_v} = 0.13 \frac{df_I}{f_I} + 5.42dA_I^* + 0.87 \frac{df_D}{f_D} + 0.89dA_D^*$	7.3%	19.4%	76.4%	-3.2%

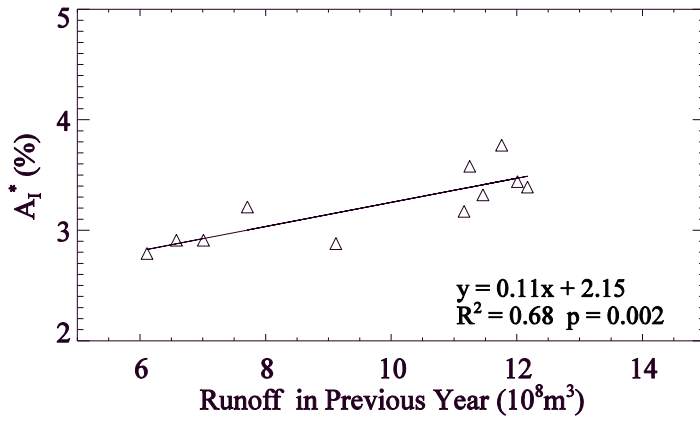


1

2

Fig. 7. Relationship between growing season desert vegetation cover (f_D) and annual precipitation (per GPCCC database 2000-2010).

3



4

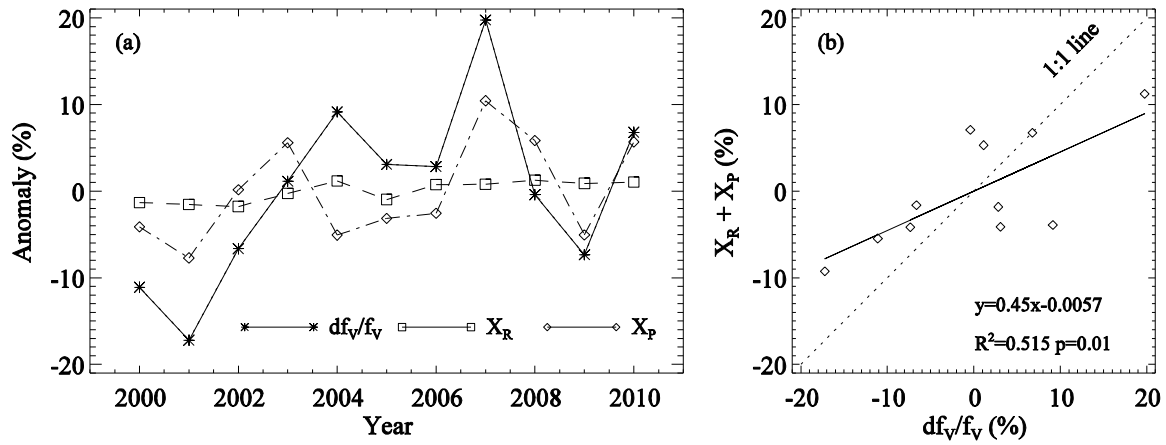
5

Fig. 8 Relationship between fractional irrigated area A_I^* and runoff at Zhengyixia from the previous year 2000-2010.

6

7

8



1

2

Fig.9 Relation between regional vegetation cover and water availability. (a) Relative variations, and (b) the observed annual changes in relative vegetation cover (df_v/f_v) versus predicted changes from water availability of runoff (X_R) and precipitation (X_P).

3

4

5
6 **Supplement:**

7

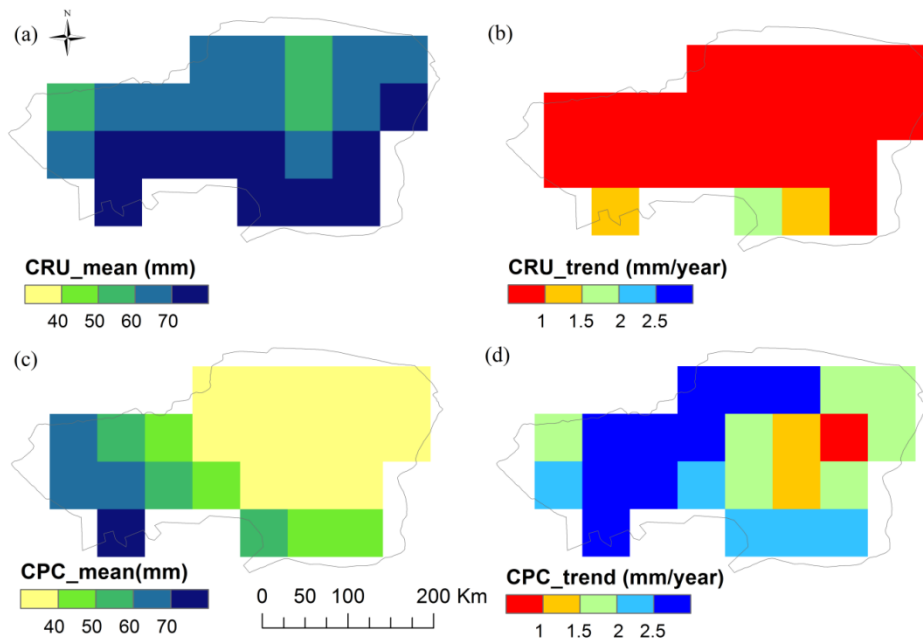
Table S1 Statistics (e.g., R^2 , significance level (p), and the slope of the linear regression)

8

between desert vegetation cover f_D and regional precipitation variations from different sources

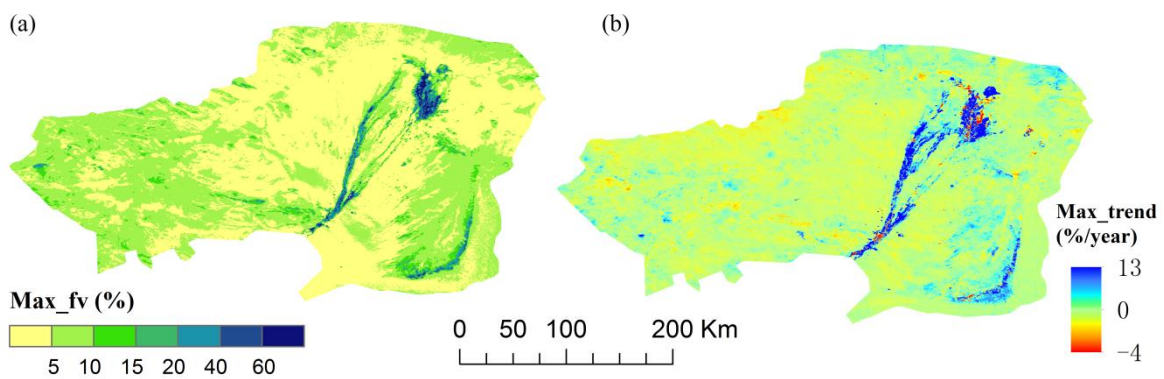
	GPCC	CRU	SITES	CPC
R^2	0.40	0.37	0.49	0.51
p	0.04	0.05	0.02	0.01
Slope	0.017	0.015	0.018	0.014

9



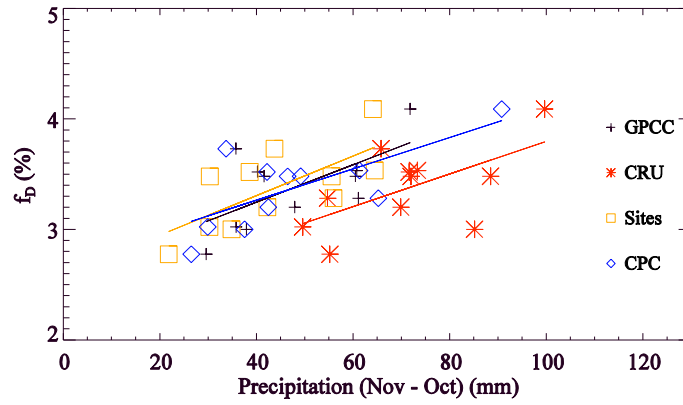
1
2
3
4
5

Fig. S1 Spatial pattern and change of precipitation for the study area from different sources. (a) Mean annual precipitation from CRU. (b) spatial trend of precipitation from CRU 2000-2010 (c) Mean annual precipitation from CPC. (d) spatial trend of precipitation from CPC 2000-2010.



6
7
8

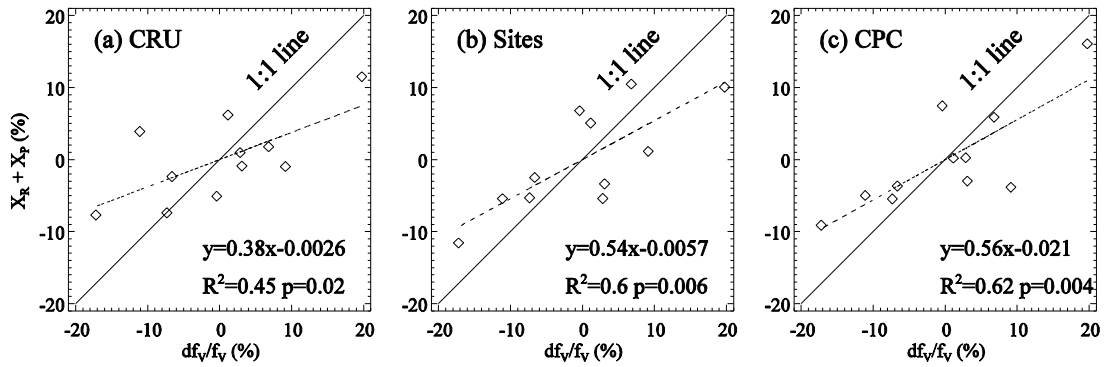
Fig. S2 Spatial of annual maximal fraction vegetation cover (a) Averaged annual max fraction vegetation cover (Max_fv) and (b) change in annual max NDVI during 2000-2012



1

2 Fig. S3 Relationship between desert vegetation cover f_D and regional precipitation from different data sets

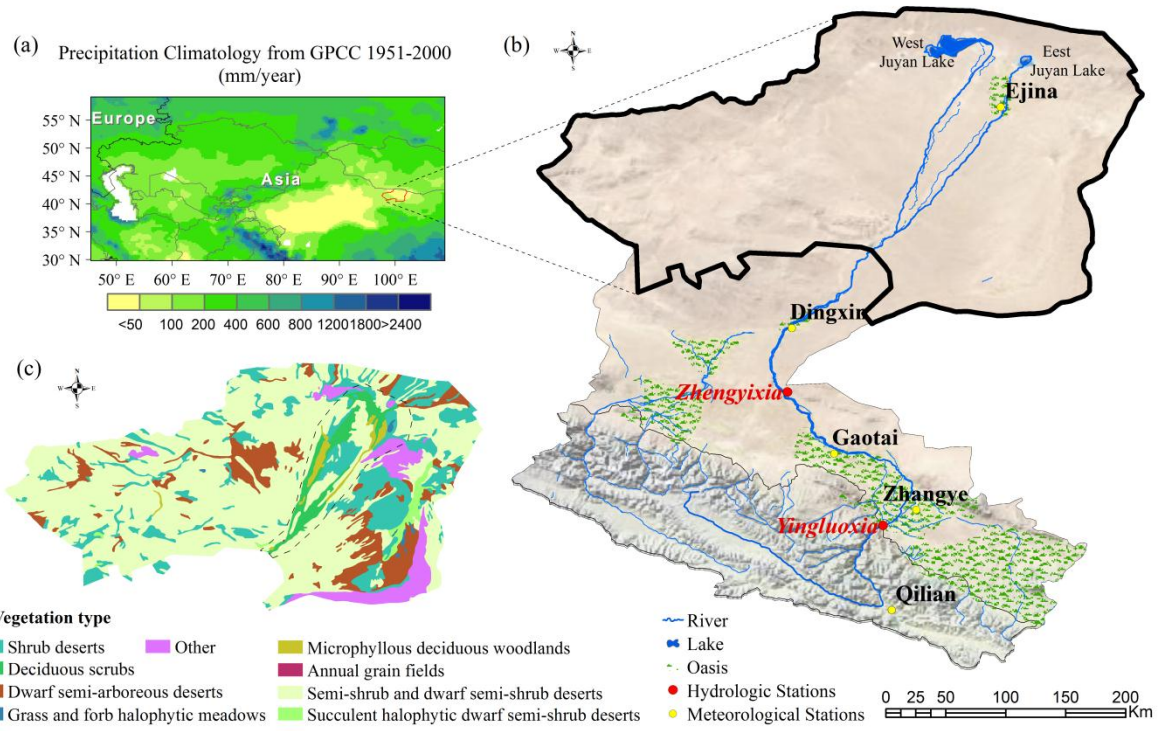
3



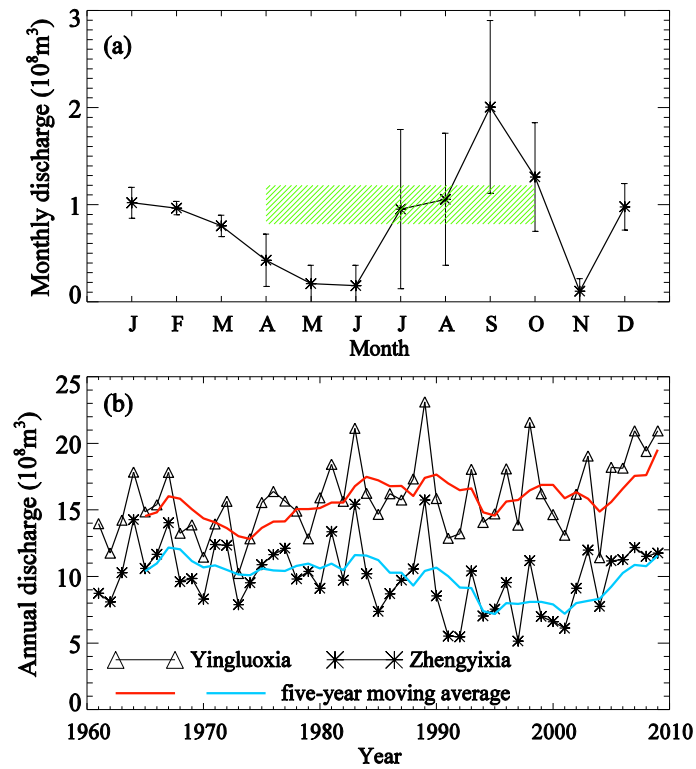
4

5 Fig.S4 The observed annual changes in relative vegetation cover (df_V/f_V) versus predicted changes from
 6 water availability of runoff (X_R) and precipitation (X_P) in relative vegetation cover with different
 7 percipitation data sources.

8



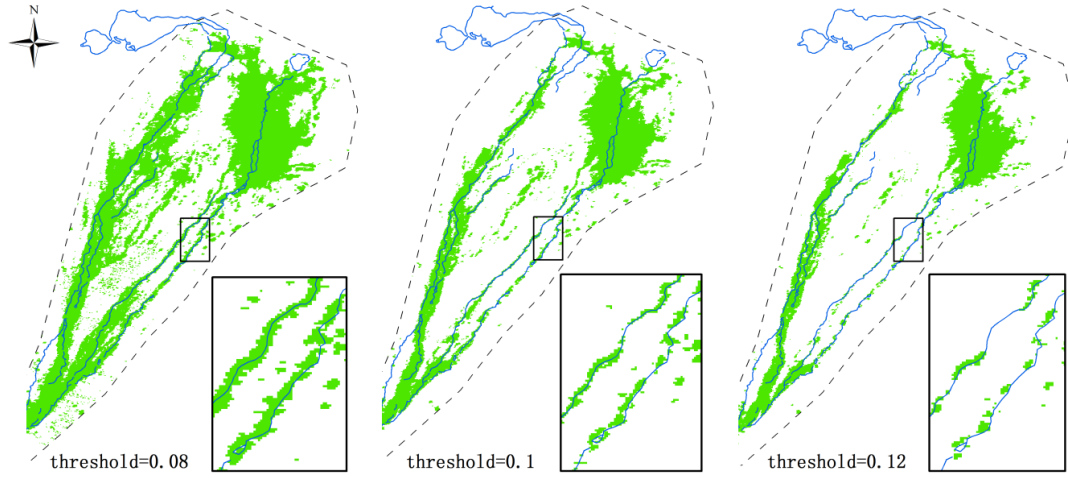
1
 2 Fig. 1 Details of the study area. (a) Regional setting and the mean annual precipitation (1951-2000). (b)
 3 Landscape of Heihe River Basin with location of meteorological and hydrologic observation sites. (c) Vegetation
 4 Map of lower Heihe river basin where the dashed line denotes the bounds of the possible irrigation area.



5

1 Fig. 2 River flows in the Heihe River basin. (a) Mean monthly river discharge (bars indicate standard deviation)
2 of Heihe River (2000-2009) at Zhengyixia station in relation to the growing season (diagonal stripes). (b) Annual
3 discharge of Heihe River (1961-2009) at Yingluoxia and Zhengyixia stations

4

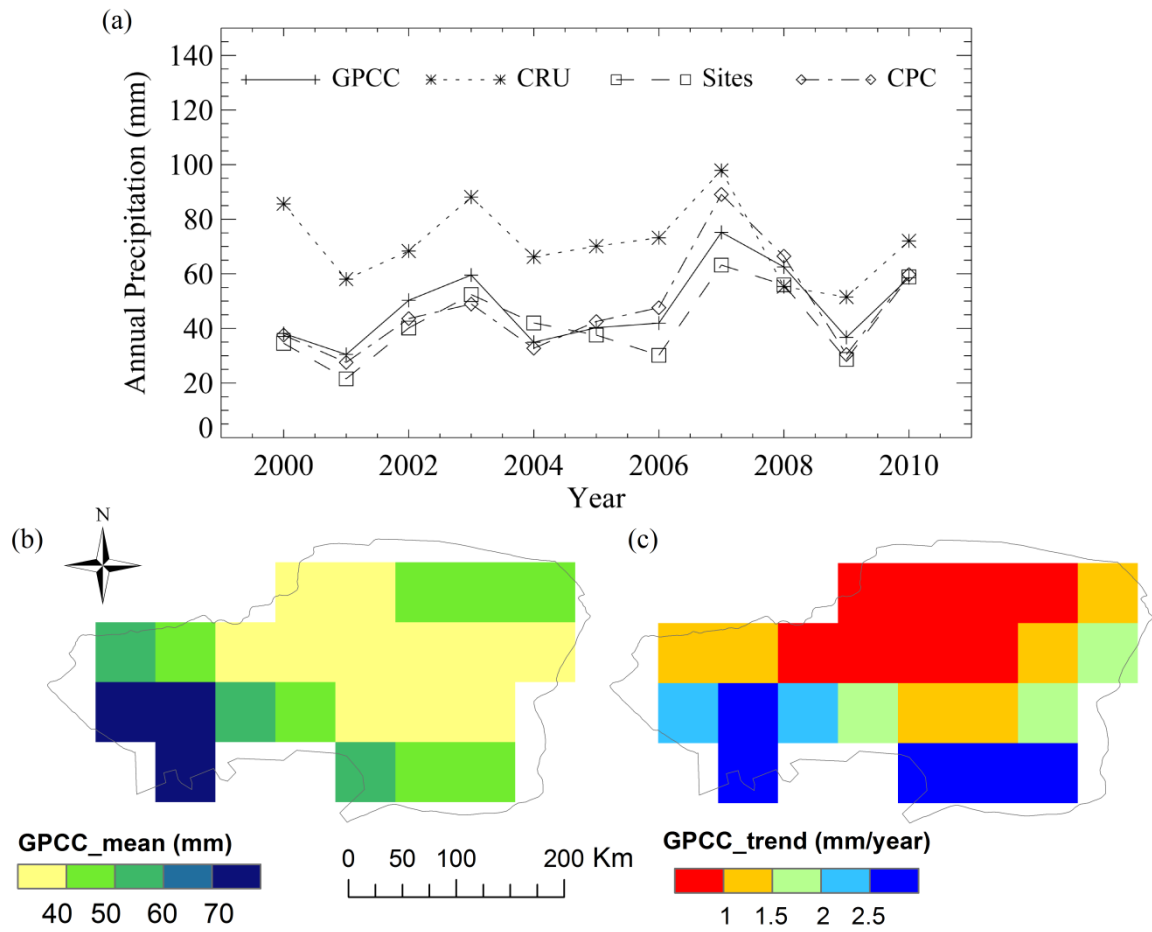


5

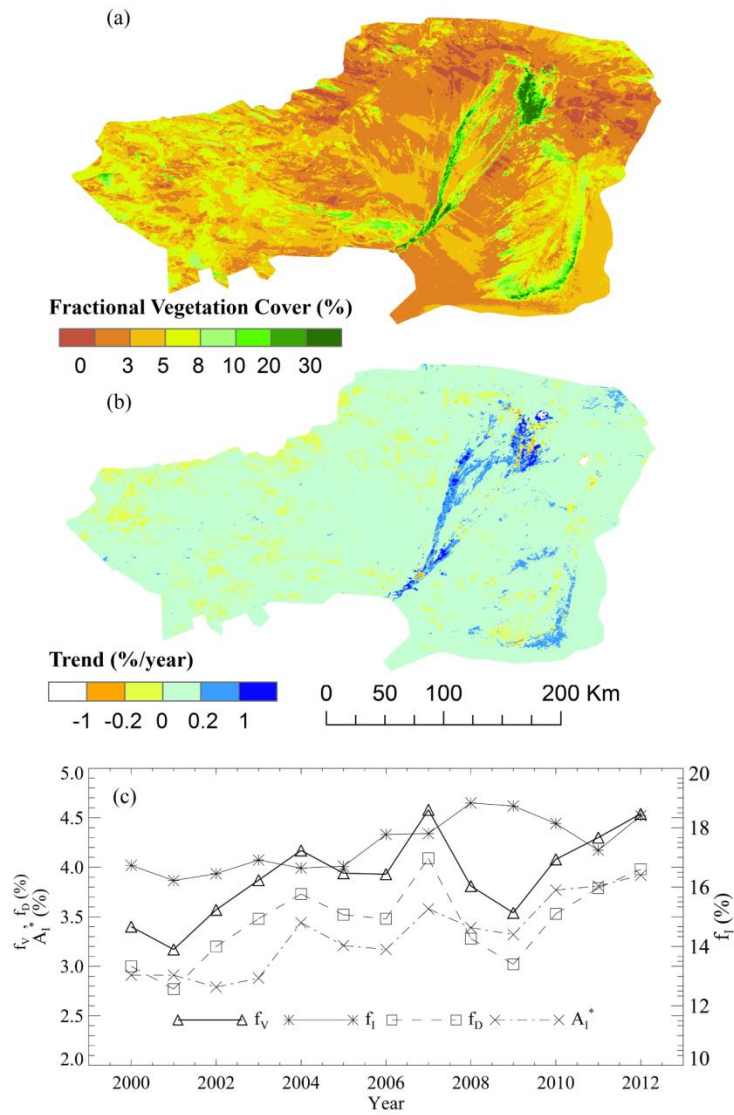
6

Fig. 3 Irrigated areas derived using different NDVI thresholds

7

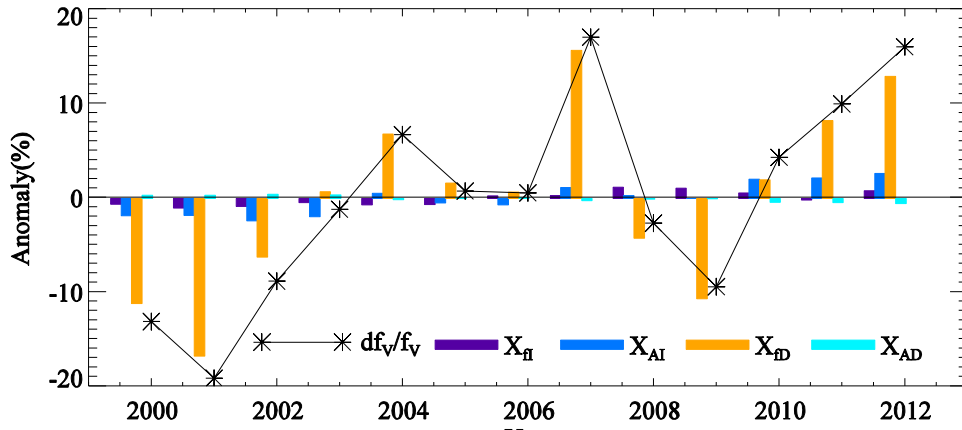


1
 2 Fig. 4 Spatial-temporal change of precipitation for the study area. (a) Annual precipitation per four different data
 3 sources (as indicated); (b) Mean annual precipitation from GPCCC, and (c) the trend from 2000 to 2010.



1
2
3
4
5
6
7

Fig. 5 Spatial-temporal change of the growing season (April-October) mean annual fractional vegetation cover (2000-2012). (a) Spatial pattern of growing season (April-October) mean annual fractional vegetation cover; (b) Spatial trend of growing season (April-October) mean annual fractional vegetation cover (2000-2012); (c) Trends in the growing season (April-October) mean annual fractional vegetation for the whole region (f_v , left scale), desert (f_D , left scale) and irrigated (f_I , right scale) land cover classes, and for the fractional area of irrigation (A_I^* , left scale).



1

2

Fig.6 Annual changes in relative vegetation cover (df_v/f_v) and the underlying components from mean annual fractional vegetation for the desert (X_{fD}) and for the irrigated (X_{fI}) regions along with changes due to changes in the fractional area of desert (X_{AD}) and irrigated (X_{AI}) regions.

5

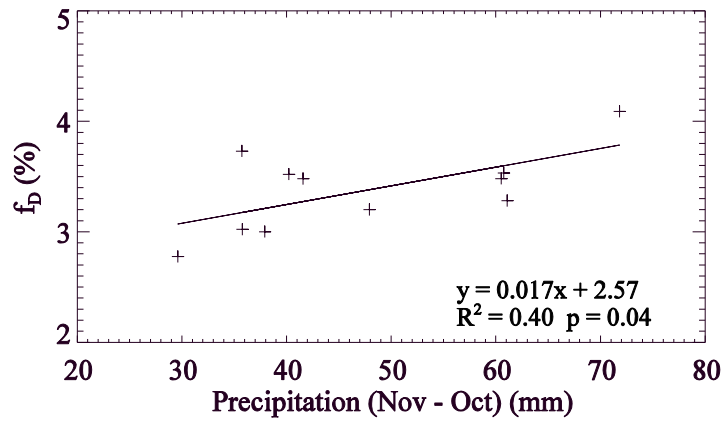
6

Table 1 Sensitivity and attribution uncertainty with varied NDVI thresholds to define irrigated and non-irrigated region (mean annual fractional vegetation for the whole region f_v , irrigated oasis f_I and desert

8

f_D , fractional area of irrigation A_I^* and desert A_D^* ; And their attribution X_{fI} , X_{AI} , X_{fD} , X_{AD})

NDVI Threshold	Sensitivity	Attribution			
		X_{fI}	X_{AI}	X_{fD}	X_{AD}
0.08	$\frac{df_v}{f_v} = 0.18 \frac{df_I}{f_I} + 2.97dA_I^* + 0.82 \frac{df_D}{f_D} + 0.88dA_D^*$	14.0%	16.8%	74.1%	-5.0%
0.09	$\frac{df_v}{f_v} = 0.16 \frac{df_I}{f_I} + 3.76dA_I^* + 0.84 \frac{df_D}{f_D} + 0.88dA_D^*$	9.5%	19.4%	75.6%	-4.5%
0.1	$\frac{df_v}{f_v} = 0.15 \frac{df_I}{f_I} + 4.45dA_I^* + 0.85 \frac{df_D}{f_D} + 0.88dA_D^*$	7.8%	20.5%	75.8%	-4.1%
0.11	$\frac{df_v}{f_v} = 0.14 \frac{df_I}{f_I} + 4.99dA_I^* + 0.86 \frac{df_D}{f_D} + 0.89dA_D^*$	7.6%	20.3%	75.7%	-3.6%
0.12	$\frac{df_v}{f_v} = 0.13 \frac{df_I}{f_I} + 5.42dA_I^* + 0.87 \frac{df_D}{f_D} + 0.89dA_D^*$	7.3%	19.4%	76.4%	-3.2%

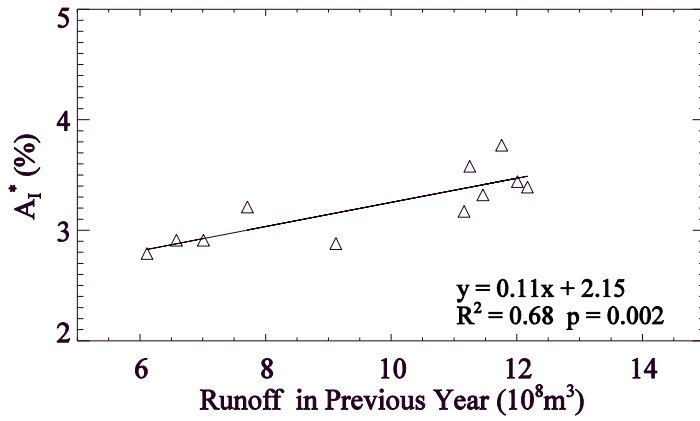


1

2

Fig. 7. Relationship between growing season desert vegetation cover (f_D) and annual precipitation (per GPCCC database 2000-2010).

3



4

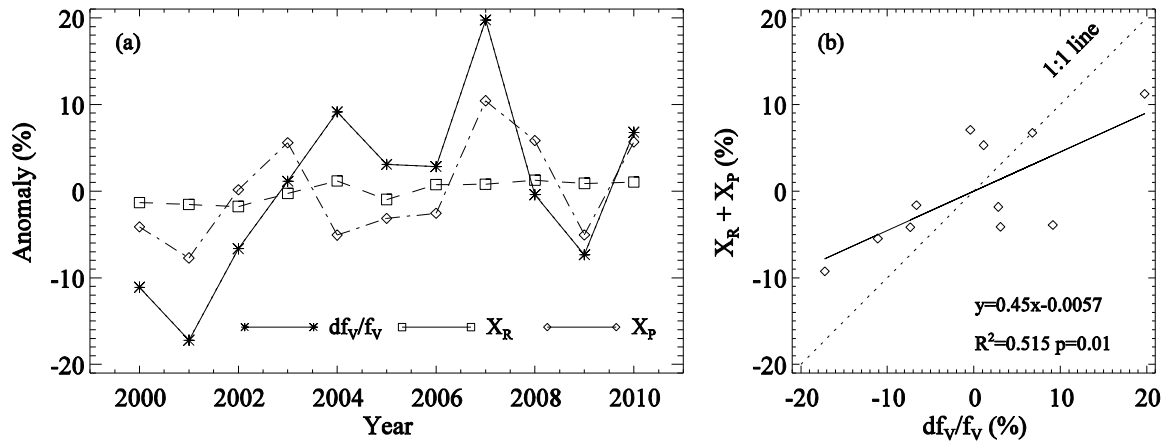
5

Fig. 8 Relationship between fractional irrigated area A_I^* and runoff at Zhengyixia from the previous year 2000-2010.

6

7

8



1

2 Fig.9 Relation between regional vegetation cover and water availability. (a) Relative variations, and (b) the
 3 observed annual changes in relative vegetation cover (df_v/f_v) versus predicted changes from water availability of
 4 runoff (X_R) and precipitation (X_P).
 5

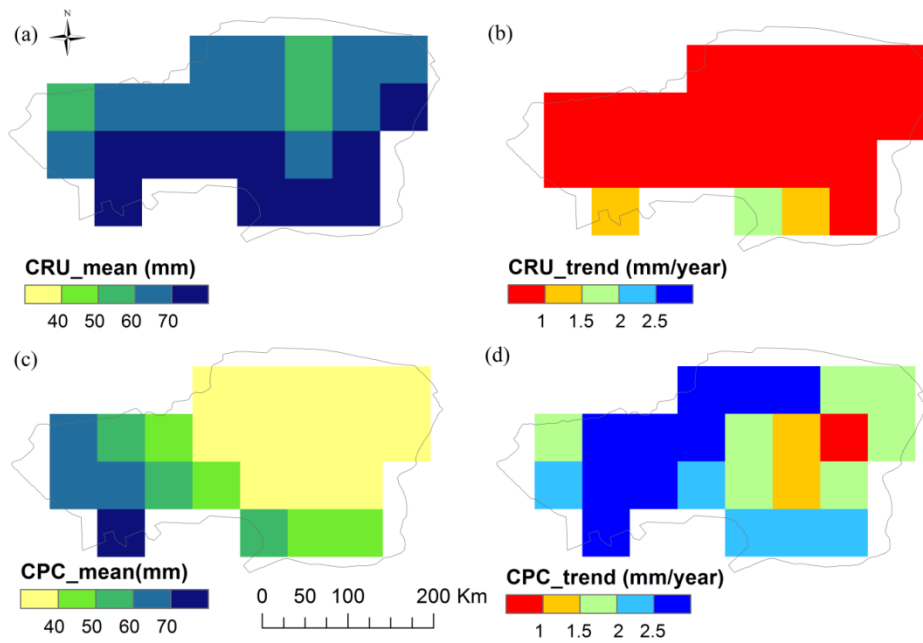
6

6 Supporting material

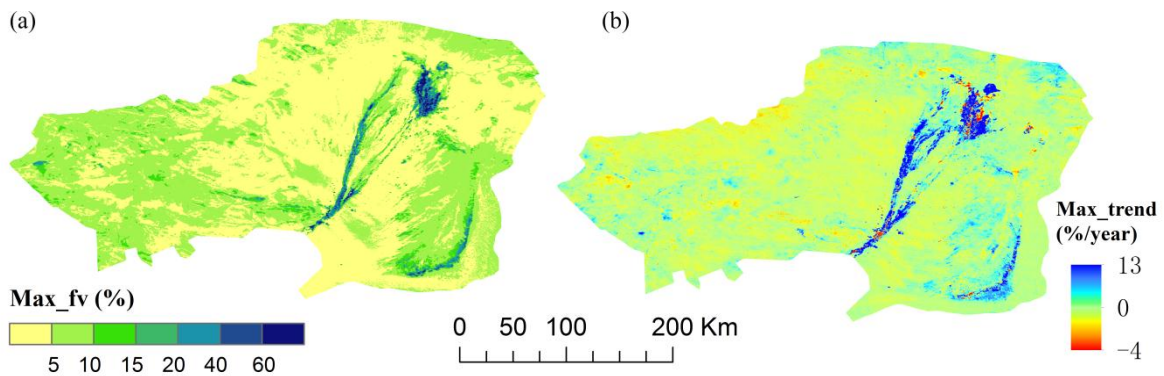
7 Table S1 Statistics (e.g., R^2 , significance level (p), and the slope of the linear regression)
 8 between desert vegetation cover f_D and regional precipitation variations from different sources

	GPCC	CRU	SITES	CPC
R^2	0.40	0.37	0.49	0.51
p	0.04	0.05	0.02	0.01
Slope	0.017	0.015	0.018	0.014

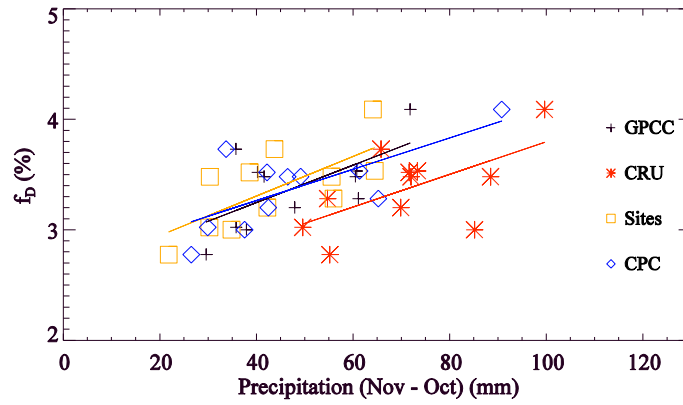
9



1
 2 Fig. S1 Spatial pattern and change of precipitation for the study area from different sources. (a)
 3 Mean annual precipitation from CRU. (b) spatial trend of precipitation from CRU 2000-2010
 4 (c) Mean annual precipitation from CPC. (d) spatial trend of precipitation from CPC
 5 2000-2010.

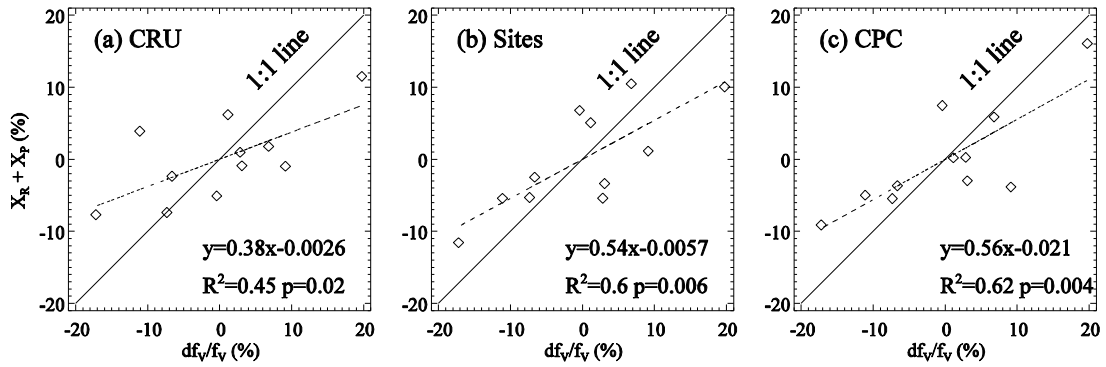


7
 8 Fig. S2 Spatial of annual maximal fraction vegetation cover (a) Averaged annual max fraction
 9 vegetation cover (Max_fv) and (b) change in annual max NDVI during 2000-2012



1
2
3
4

Fig. S3 Relationship between desert vegetation cover f_D and regional precipitation from different data sets



5
6
7
8
9

Fig.S4 The observed annual changes in relative vegetation cover (df_V/f_V) versus predicted changes from water availability of runoff (X_R) and precipitation (X_P) in relative vegetation cover with different precipitation data sources.